

# Understanding the influence of HEPES buffer concentration on the biodegradation of pure magnesium: An electrochemical study

**M. Bobby Kannan<sup>\*,†,‡</sup>, Hadis Khakbaz<sup>†</sup>, A. Yamamoto<sup>‡</sup>**

<sup>†</sup>*Biomaterials and Engineering Materials (BEM) Laboratory, College of Science, Technology and Engineering, James Cook University, Townsville, Queensland 4811, Australia*

<sup>‡</sup>*Biometals Group, International Centre for Materials Nanoarchitectonics, National Institute for Materials Science, Tsukuba, Ibaraki 305-0044, Japan*

## ABSTRACT

A systematic electrochemical study was performed to understand the influence of HEPES buffer concentration on the biodegradation behaviour of pure magnesium in a pseudo-physiological solution (Earle's balanced salt solution (EBSS)). Electrochemical impedance spectroscopy (EIS) and potentiodynamic polarisation experiments suggest that HEPES accelerates the degradation of magnesium. While 5%CO<sub>2</sub> in EBSS reduced the polarisation resistance ( $R_p$ ) of magnesium by ~79%, addition of HEPES (25mM) to EBSS decreased the  $R_p$  of magnesium by ~98% and escalated the corrosion current ( $i_{\text{corr}}$ ) by over an order of magnitude as compared to that in EBSS. Increase in HEPES concentration, i.e., 50 mM and 100 mM, further increased the degradation of magnesium. Interestingly, the bulk pH of the test solution before and after the electrochemical testing, was not significantly different with the addition of HEPES concentration or presence of CO<sub>2</sub> in EBSS. However, the anodic polarisation curves suggest that higher HEPES concentration inhibited the formation of insoluble salt layer on the surface of magnesium which influences its

degradation behaviour. These findings clearly indicate that carbonate buffer system and 5% CO<sub>2</sub> atmosphere is essential for evaluating the degradation behaviour of magnesium-based materials, and is not replaceable by addition of HEPES addition.

**KEYWORDS:** *Magnesium, Biomaterials, Degradation, HEPES, Earle's balanced salt solution (EBSS)*

## **INTRODUCTION**

In vitro degradation behaviour of magnesium-based materials for biodegradable implant applications has been widely studied over the past decade [1-14]. Typically, simple immersion and electrochemical techniques in a pseudo-physiological solution have been used to evaluate the in vitro degradation behaviour of magnesium-based materials [2-14]. There are a few recipes for pseudo-physiological solution, which mimic the actual physiological solution [12,15,16]. Broadly, pseudo-physiological solutions can be classified into two groups: (i) solutions utilizing carbonate buffer system [e.g., Earle's Balanced Salt Solution (EBSS), Eagle's Minimum Essential Medium (EMEM) and Dulbecco's Modified Eagle Medium (DMEM)], and (ii) solutions not utilizing carbonate buffer system [e.g., Hanks' Balanced Salt Solution (HBSS), and simulated body fluid (SBF)]. Table 1 shows the chemical composition of the most common pseudo- physiological solutions which have been used to evaluate the in vitro degradation behaviour of magnesium-based materials. It should be noted that the pH of the body fluid is mainly controlled by carbonate buffer system [17]. The buffering capacity of carbonate buffer system depends on the amount of bicarbonate and the partial pressure of carbon dioxide (CO<sub>2</sub>), since dissolved CO<sub>2</sub> forms carbonic

acid [17]. The human arterial CO<sub>2</sub> pressure is about 40 Torr [18], which is much higher than that in the atmospheric air (~0.3 Torr). This indicates that pseudo-physiological solutions with carbonate buffer system require relatively higher CO<sub>2</sub> atmosphere (ca. 5%) to fully simulate the buffering ability of the body fluid. However, for experimental simplicity, buffers such as HEPES (2-(4-(2-hydroxyethyl)-1-piperazinyl) ethanesulfonic acid) and TRIS (tris(hydroxymethyl)aminomethane) are added to the pseudo-physiological solutions as a substitute to carbonate buffer system to maintain the pH of the solution.

Table 2 shows some quantitative data, such as corrosion current ( $i_{\text{corr}}$ ), corrosion potential ( $E_{\text{corr}}$ ), and polarisation resistance ( $R_p$ ) on the degradation of pure magnesium in different pseudo-physiological solutions [7, 14, 19-26]. The degradation behaviour of magnesium appears to be depended on the type of the pseudo-physiological solution used. Generally, the difference in the degradation behaviour can be attributed to various factors such as the purity of metal, chemical composition of the solution, static/dynamic condition of the solution during testing, and also sample surface preparation. However, magnesium being a highly electronegative metal and has a high tendency to dissolve in aqueous solution very rapidly, the chemical composition of the pseudo-physiological solution will play a significant role. For evaluating the degradation of magnesium-based materials, buffer system is critical since magnesium dissolution will increase the pH of the electrolyte which does not simulate the physiological condition. Furthermore, under high pH condition magnesium will tend to passivate and as a result the degradation rate measured from the in vitro testing will be lower than under in vivo condition.

HEPES buffer has been widely used in the in vitro degradation studies of magnesium-based materials [2, 21, 22, 27, 28]. HEPES, as shown in Fig. 1, is a zwitterionic buffer which is often added to cell culture medium to maintain a physiological pH of 7.4 exposed to atmospheric air.

However, the HEPES concentration used in the pseudo-physiological solutions is quite high, i.e., ~18-24 g/l [2, 11, 29], as compared to the other constituents in the solution. Hence, it is necessary to know if the recommended large amounts of HEPES buffer influence the magnesium degradation apart from maintaining the pH of the solution.

In general, studies on the effect of buffers on the dissolution behaviour of magnesium are scarce. Recently, Dezfuli et al.[20] and Kirkland et al.[29] reported that HEPES buffer accelerates the degradation of magnesium. Dezfuli et al.[20] stated that HEPES retains the local pH of the solution and hence increase the degradation of magnesium. But it should be noted that the local pH change reported by the authors for magnesium without HEPES is not significantly high (initial pH ~7.45 and final pH ~7.65 (3600s exposure) to cause passivation. The authors also reported that HEPES reduced the precipitation of calcium phosphate on magnesium. Kirkland et al. suggested interaction or complex formation between HEPES and magnesium causing the increased degradation.

In order to understand the influence of HEPES on the degradation mechanism of magnesium, the HEPES concentration effect in the pseudo-physiological solution should be analysed. Hence, in this study, a systematic approach has been taken to understand the influence of HEPES buffer concentration on magnesium degradation. Electrochemical experiments and microscopy analysis have been carried out to elucidate the mechanism of magnesium degradation in the presence of HEPES.

## **MATERIALS AND METHODS**

The degradation behaviour of pure magnesium (chemical composition is given in Table 3) was studied in EBSS with or without three different concentrations of HEPES, i.e., 25, 50 and 100 mM,

at 37°C using electrochemical techniques. In order to investigate the pH change due to magnesium dissolution and the effectiveness of the HEPES buffer, a relatively small electrochemical cell as shown in Fig. 2 was used in this study. The electrochemical cell consisted of a standard three-electrode system, i.e., a sample (0.95 cm<sup>2</sup> exposed area) as a working electrode, Ag/AgCl (3M NaCl) as a reference electrode and a platinum mesh as a counter electrode, with an electrolyte volume of 10 ml. The electrochemical cell was housed in a CO<sub>2</sub> incubator (Model: APC-30D, ASTEC Co. Ltd., Fukuoka, Japan) to maintain the temperature at 37°C. In one of the experimental conditions, the atmosphere in the incubator was controlled to be 5% CO<sub>2</sub> in humidified air to simulate the physiological condition (referred as EBSS+CO<sub>2</sub>). The electrochemical experiments were conducted using a potentiostat/frequency response analyser (Model: VersaSTAT3, Princeton Applied Research, Oak Ridge, USA).

Prior to the electrochemical testing, the magnesium samples were ground with SiC paper up to 2500 grit and followed by ultrasonic cleaning in acetone and then in ethanol. Electrochemical impedance spectroscopy (EIS) experiments were performed at open circuit potential with AC amplitude of 5 mV over the frequency range of 10<sup>5</sup> Hz to 10<sup>-2</sup> Hz. The EIS plots were modelled using ZSimpWin 3.21 software. Potentiodynamic polarisation experiments were conducted at a scan rate of 0.5 mV/s. The samples were exposed to the medium for 2 h to establish a relatively stable open circuit potential before commencing the electrochemical testing.

## RESULTS

The Nyquist plots of pure magnesium in EBSS, EBSS+CO<sub>2</sub>, and EBSS with different concentrations of HEPES are shown in Fig. 3. The equivalent circuit used to model the EIS spectra is shown as an inset in Fig 3, and the modelling results are presented in Table 4. CPE<sub>1</sub> represents

the double layer capacitance,  $R_1$  the charge transfer resistance;  $CPE_2$  and  $R_2$  represent the film effects [31]. The polarisation resistance ( $R_p$ ) was calculated by adding  $R_1$  and  $R_2$ , and presented in Fig.4. The EIS results suggest that addition of HEPES decreases the  $R_p$  of magnesium significantly. EBSS+  $CO_2$  decreased the  $R_p$  of magnesium by  $\sim 79\%$  as compared that of in EBSS only ( $R_p$  in EBSS =  $46325 \Omega \text{ cm}^2$  and  $R_p$  in EBSS+ $CO_2$  =  $9862 \Omega \text{ cm}^2$ ). Interestingly, addition of 25mM of HEPES to EBSS reduced the  $R_p$  of magnesium by  $\sim 98\%$ , i.e.,  $R_p$  in EBSS + 25 mM HEPES =  $1053 \Omega \text{ cm}^2$ . Increase in HEPES concentration further reduced the  $R_p$  of magnesium, i.e.,  $R_p$  in EBSS + 50 mM HEPES =  $143 \Omega \text{ cm}^2$ , which is more than two-order of magnitude lower as compared to that in EBSS. Further increasing HEPES concentration to 100 mM reduced the  $R_p$  to  $90 \Omega \text{ cm}^2$ .

Figure 5 shows the potentiodynamic polarization curves of pure magnesium in EBSS, EBSS+ $CO_2$  and EBSS with different concentrations of HEPES. The corresponding electrochemical parameters are presented in Table 5. The cathodic current curve of magnesium moved towards the higher side in the presence of  $CO_2$ . The shift in the curves was higher when HEPES was added to EBSS, and it increased with increase in HEPES concentration. In EBSS, a passive-like anodic current curve and also a breakdown potential  $\sim -1.4 \text{ V}$  were observed. In the presence of  $CO_2$ , the anodic curve shifted towards higher current, but the breakdown potential was not changed significantly. With the addition of 25mM HEPES, a further shift in the anodic curve towards higher current was observed. Interestingly, increase in HEPES concentration made the breakdown potential to disappear. At 100mM HEPES, the breakdown potential completely disappeared and the anodic current was significantly higher than that without HEPES. The corrosion current ( $i_{\text{corr}}$ ) calculated based on the cathodic curves suggests that  $CO_2$  presence increased the  $i_{\text{corr}}$  significantly as compared to that in EBSS (i.e., EBSS =  $1.03 \mu\text{A}/\text{cm}^2$  and EBSS+ $CO_2$  =  $6.25 \mu\text{A}/\text{cm}^2$ ). Addition of

25mM HEPES to EBSS increased the  $i_{\text{corr}}$  by more than an order of magnitude (25mM HEPES = 28.5  $\mu\text{A}/\text{cm}^2$ ). Increase in HEPES concentration, i.e., 50mM and 100mM, further increased the  $i_{\text{corr}}$  (50mM HEPES = 166  $\mu\text{A}/\text{cm}^2$  and 100mM HEPES = 244  $\mu\text{A}/\text{cm}^2$ ).

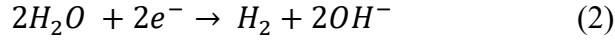
Figures 6 and 7 show the SEM micrographs of post-degraded samples. It is clearly evident that addition of  $\text{CO}_2$  and HEPES increased the degradation of magnesium as compared to that in EBSS. In EBSS, magnesium underwent very little localized degradation (Fig. 6). However, presence of  $\text{CO}_2$  in EBSS has increased the localized attack, where a large number of pits can be observed (Fig. 6). Addition of HEPES to EBSS has dramatically increased the localized attack of magnesium (Fig.7). Also, the degree of localized attack intensified with the increase in HEPES concentration. A higher magnification reveals mud-cracking in all the samples exposed to EBSS containing HEPES.

## DISCUSSION

The electrochemical results showed that HEPES accelerates the degradation of magnesium. The degradation rate measured from potentiodynamic polarisation results are presented in Fig. 8. Addition of HEPES increased the degradation rate by one-order magnitude (25mM) and two-order magnitude (50mM and 100mM) as compared to EBSS without HEPES. Notably, the degradation rate of magnesium in EBSS+HEPES was higher than in EBSS+ $\text{CO}_2$ . The observations were consistent with the EIS results and post-degradation analysis.

Dezfuli et al. [22] argued that the local pH change contributes to the degradation of magnesium. In order to understand the pH change, the pH of the solution before and after the potentiodynamic polarisation experiments were measured and presented in Table 6. The initial pH (before the experiment) was similar at  $\sim 7.4$  under all condition, i.e., EBSS, EBSS+ $\text{CO}_2$  and EBSS+HEPES.

After the potentiodynamic polarisation experiments the pH increased slightly in all those conditions, which is due to magnesium dissolution as shown below:



However, the pH difference between EBSS, EBSS+CO<sub>2</sub> and EBSS+HEPES after polarisation was not significantly high to cause the drastic difference in the degradation behaviour observed in the electrochemical experiments. To further understand the degradation mechanism of magnesium under these conditions, the pH values and the electrochemical potentials data were mapped on magnesium Pourbaix diagram (Fig.9). Interestingly, it was noticed that in all the conditions the electrochemical potentials of magnesium fall in the active region, before and after the potentiodynamic polarisation experiments. However, potentiodynamic polarisation curves suggests that the acceleration effect of HEPES on magnesium degradation is not simply explained by the marginal pH shift of the solution.

The ionic strength ( $\mu$ ) and activity coefficient ( $\gamma$ ) of the solution will have an influence on the precipitation behavior and hence the degradation tendency of the metal. Equations 3 & 4, shown below, were used to calculate  $\mu$  and  $\gamma$  based on inorganic salts in the solutions:

$$\mu = 1/2 \sum C n^2 \quad (3)$$

$$-\log \gamma = 0.5 n^2 \sqrt{\mu} \quad (4)$$

where C is the molar concentration of individual species and  $n$  is the number of moles of electrons transferred in the half reaction.

The ionic strength of EBSS was 0.16, but when HEPES was added in three different concentrations (25, 50 and 100 mM) to the EBSS, the ionic strength increased as 0.20, 0.26, and 0.36, respectively. This clearly indicates that addition of HEPES drastically increase ionic strength more than 25%. Since increase in ionic strength decreases the activity of ions in the solution, it results in the increase of insoluble salt solubility. Accompanying to magnesium dissolution, generation of hydroxide ions results in the increase of local pH and precipitation of insoluble salts such as hydroxide, carbonate and phosphate of magnesium and calcium. Increase in ionic strength reduces activity of these ions, thereby precipitation of these insoluble salts is inhibited. Thus, the addition of HEPES causes significant increase in ionic strength and decrease in ion activities. It can be noticed that as the HEPES concentration increased to 100mM the pseudo-passivation completely disappeared. This infers that the inhibition in the formation of insoluble salt layer at the magnesium surface has affected the dissolution of magnesium. At low concentration of HEPES (25mM), the reduction of ion activities was moderate which would have caused the pseudo-passivation. When 50mM HEPES was added, the pseudo-passivation largely reduced and it completely disappeared at 100mM HEPES. Higher concentration of HEPES reduces ion activities more severely, results in higher inhibition of insoluble salt layer formation. Thus, the results clearly suggest that addition of HEPES significantly influences the degradation process of magnesium, which is related to ionic strength of the solution.

## **CONCLUSION**

In vitro electrochemical study suggests that HEPES buffer has a significant effect on the degradation of magnesium. Addition of HEPES to EBSS solution increased the degradation rate of magnesium. Notably, the degradation rate of magnesium in HEPES containing medium was significantly higher than in EBSS+CO<sub>2</sub>. The pH of the bulk solution before and after the

potentiodynamic polarisation experiments did not change significantly under all conditions (EBSS, EBSS+HEPES, EBSS+CO<sub>2</sub>) to cause such a drastic difference in the degradation behaviour. The study suggests that the increase in ionic strength due to HEPES addition and consequent decrease in ion activities inhibited the insoluble salt layer formation on magnesium. These findings indicate that HEPES is not a suitable buffer to substitute carbonate buffer system containing 5% CO<sub>2</sub> for evaluating the degradation behaviour of magnesium-based materials.

## AUTHOR INFORMATION

### Corresponding Author

\*E-mail: bobby.mathan@jcu.edu.au.

### Notes

The authors declare no competing financial interest.

## ACKNOWLEDGMENT

The authors would like to thank the National Institute for Materials Science (NIMS) for the MANA Short Term Research Program and JSPS KAKENHI (Grant number 26282151) for partial financial support.

## REFERENCES

- (1) Zheng, Y.; Gu, X.; Witte, F. Biodegradable metals. *Mater. Sci. Eng., R* **2014**, 77, 1-34.
- (2) Kannan, M.B.; Raman, R.S. In vitro degradation and mechanical integrity of calcium-containing magnesium alloys in modified-simulated body fluid. *Biomaterials* **2008**, 29(15), 2306-2314.
- (3) Singer, F.; Schlesak, M.; Mebert, C.; Hohn, S.; Virtanen, S. Corrosion Properties of Polydopamine Coatings Formed in One-Step Immersion Process on Magnesium. *ACS Appl. Mater. Interfaces* **2015**, 7(48), 26758-26766.

- (4) Kannan, M.B. Influence of microstructure on the in-vitro degradation behaviour of magnesium alloys. *Mater. Lett.* **2010**, 64(6), 739-742.
- (5) Chen, Y.; Zhao, S.; Liu, B.; Chen, M.; Mao, J.; He, H.; Zhao, Y.; Huang, N.; Wan, G. Corrosioncontrolling and osteo-compatible Mg ion-integrated phytic acid (Mg-PA) coating on magnesium substrate for biodegradable implants application. *ACS Appl. Mater. Interfaces* **2014**, 6(22), 19531-19543.
- (6) Walter, R.; Kannan, M.B. A mechanistic in vitro study of the microgalvanic degradation of secondary phase particles in magnesium alloys. *J. Biomed. Mater. Res., part A* **2015**, 103(3), 990-1000.
- (7) Gu, X.; Zheng, Y.; Cheng, Y.; Zhong, S.; Xi, T. In vitro corrosion and biocompatibility of binary magnesium alloys. *Biomaterials* **2009**, 30(4), 484-498.
- (8) Walter, R.; Kannan, M.B. In-vitro degradation behaviour of WE54 magnesium alloy in simulated body fluid. *Mater. Lett.* **2011**, 65(4), 748-750.
- (9) Kannan, M.B.; Yamamoto, A.; Khakbaz, H. Influence of living cells (L929) on the biodegradation of magnesium–calcium alloy. *Colloids Surf., B* **2015**, 126, 603-606.
- (10) Schinhammer, M.; Hofstetter, J.; Wegmann, C.; Moszner, F.; Loffler, J.F.; Uggowitzer, P.J. On the immersion testing of degradable implant materials in simulated body fluid: active pH regulation using CO<sub>2</sub>. *Adv. Eng. Mater.* **2013**, 15(6), 434-441.
- (11) Hanzi, A.C.; Gerber, I.; Schinhammer, M.; Loffler, J.F.; Uggowitzer, P.J. On the in vitro and in vivo degradation performance and biological response of new biodegradable Mg–Y–Zn alloys. *Acta Biomater.* **2010**, 6(5), 1824-1833.
- (12) Yamamoto, A.; Hiromoto, S. Effect of inorganic salts, amino acids and proteins on the degradation of pure magnesium in vitro. *Mater. Sci. Eng., C* **2009**, 29(5), 1559-1568.
- (13) Kannan, M.B.; Walter, R.; Yamamoto, A. Biocompatibility and in Vitro Degradation Behavior of Magnesium–Calcium Alloy Coated with Calcium Phosphate Using an Unconventional Electrolyte. *ACS Biomater. Sci. Eng.* **2015**, 2(1), 56-64.
- (14) Khakbaz, H.; Walter, R.; Gordon, T.; Kannan, M.B. Self-dissolution assisted coating on magnesium metal for biodegradable bone fixation devices. *Mater. Res. Express* **2014**, 1(4), 045406.
- (15) Oyane, A.; Kim, H.M.; Furuya, T.; Kokubo, T.; Miyazaki, T.; Nakamura, T. Preparation and assessment of revised simulated body fluids. *J. Biomed. Mater. Res., part A* **2003**, 65(2), 188-195.
- (16) Bohner, M.; Lemaitre, J. Can bioactivity be tested in vitro with SBF solution? *Biomaterials* **2009**, 30(12), 2175-2179.
- (17) Mohan, C. *Buffers. A Guide for the Preparation and Use of Buffers in Biological Systems.* **2003**, Darmstadt: Calbiochem. 1-29.

- (18) Kanai, I.; Kanai, M. *Kanai's Manual of Clinical Laboratory Medicine*. 31 ed. **1998**, Kinbarashuppan, Tokyo. 702-708.
- (19) Chen, X.-B.; Birbilis, N.; Abbott, T. A simple route towards a hydroxyapatite–Mg(OH)<sub>2</sub> conversion coating for magnesium. *Corros. Sci.* **2011**, 53(6), 2263-2268.
- (20) Degner, J.; Singer, F.; Cordero, L.; Boccaccini, A.R.; Virtanen, S. Electrochemical investigations of magnesium in DMEM with biodegradable polycaprolactone coating as corrosion barrier. *Appl. Surf. Sci.* **2013**, 282, 264-270.
- (21) Kirkland, N.T.; Birbilis, N.; Staiger, M.P. Assessing the corrosion of biodegradable magnesium implants: A critical review of current methodologies and their limitations. *Acta Biomater.* **2012**, 8(3), 925-936.
- (22) Naddaf Dezfuli, S.; Huan, Z.; Mol, J.M.C.; LeeFlang, M.A.; Chang, J.; Zhou, J. Influence of HEPES buffer on the local pH and formation of surface layer during in vitro degradation tests of magnesium in DMEM. *Progress in Natural Science: Materials International* **2014**, 24(5), 531-538.
- (23) Jo, J.-H.; Hong, J.-Y.; Shin, K.-S.; Kim, H.-E.; Koh, Y.-H. Enhancing biocompatibility and corrosion resistance of Mg implants via surface treatments. *J. Biomater. Appl.* **2012**, 27(4), 469-476.
- (24) Chiu, K.; Wong, M.; Cheng, F.; Man, H. Characterization and corrosion studies of fluoride conversion coating on degradable Mg implants. *Surf. Coat. Technol.* **2007**, 202(3), 590-598.
- (25) Xin, Y.; Hu, T.; Chu, P.K. Degradation behaviour of pure magnesium in simulated body fluids with different concentrations of. *Corros. Sci.* **2011**, 53(4), 1522-1528.
- (26) Ng, W.; Wong, M.; Cheng, F. Stearic acid coating on magnesium for enhancing corrosion resistance in Hanks' solution. *Surf. Coat. Technol.* **2010**, 204(11), 1823-1830.
- (27) Kannan, M.B.; Orr, L. In vitro mechanical integrity of hydroxyapatite coated magnesium alloy. *Biomed. Mater.* **2011**, 6(4), 045003.
- (28) Choudhary, L.; Raman, R.S. Mechanical integrity of magnesium alloys in a physiological environment: slow strain rate testing based study. *Eng. Fract. Mech.* **2013**, 103, 94-102.
- (29) Seitz, J.M.; Collier, K.; Wulf, E.; Bormann, D.; Bach, F.W. Comparison of the corrosion behavior of coated and uncoated magnesium alloys in an in vitro corrosion environment. *Adv. Eng. Mater.* **2011**, 13(9), B313-B323.
- (30) Kirkland, N.T.; Waterman, J.; Birbilis, N.; Dias, G.; Woodfield, T.B.; Hartshorn, R.M.; Staiger, M.P. Buffer-regulated biocorrosion of pure magnesium. *J. Mater. Sci. - Mater. Med.* **2012**, 23(2), 283-291.
- (31) Alabbasi, A.; Bobby Kannan, M.; Walter, R.; Stormer, M.; Blawert, C. Performance of pulsed constant current silicate-based PEO coating on pure magnesium in simulated body fluid. *Mater. Lett.* **2013**, 106, 18-21.



**Table 1.** Ion Concentrations of blood plasma and different pseudo-physiological solutions.

<b>Composition</b>	<b>Blood Plasma [14]</b>	<b>SBF [14]</b>	<b>HBSS [*]</b>	<b>EBSS [*]</b>	<b>EMEM [**]</b>	<b>DMEM [*]</b>
Na <sup>+</sup> (mM)	142	142	141.8	143.5	143.5	127.3
K <sup>+</sup> (mM)	5	5	5.37	5.37	5.37	5.3
Mg <sup>2+</sup> (mM)	1.5	1.5	.081	0.81	0.81	0.8
Ca <sup>2+</sup> (mM)	2.5	2.5	1.3	1.80	1.80	1.8
Cl <sup>-</sup> (mM)	103	147.8	.1448	123.5	124.7	90.8
HCO <sub>3</sub> <sup>-</sup> (mM)	27	4.2	4.2	26.2	26.2	44.1
HPO <sub>4</sub> <sup>2-</sup> (mM)	1	1	0.77	0.90	0.90	0.9
SO <sub>4</sub> <sup>2-</sup> (mM)	0.5	0.5	0.81	0.81	0.81	0.8
Glucose (g/L)	~1.1	-	1	1	1	4.5
Amino acids and vitamins (g/L)	0.25-0.4	-	-	-	0.81	1.64
Proteins (g/L)	63-80	-	-	-	-	-
Phenol red (g/L)	-	-	0.017	0.017	0.006	0.015

\*MP Bio, 1810049 (HBSS), 1800049(EBSS), and 1033122(DMEM)

\*\* Eagle's MEM "Nissui", Nissui Pharmaceutical Co Ltd. Tokyo, Japan

**Table 2.** Electrochemical degradation data of pure magnesium in different pseudo-physiological solutions.

Media	atmosphere	Buffer	$i_{\text{corr}}$ ( $\mu\text{A}/\text{cm}^2$ )	$E_{\text{corr}}$ (V)	$R_p$ ( $\Omega.\text{cm}^2$ )
Hanks [5]	air		15.98	-1.53 (SCE)	
MEM [17]	5% CO <sub>2</sub>		600	-1.6 (SCE)	
DMEM [18]	air		3 (15 min)	-1.58 (15 min) (Ag/AgCl)	
Hanks [19]		HEPES	30	-1.94 (SCE)	432
DMEM [20]	air	HEPES		-1.77 (SCE)	
SBF [5]	air	Tris	86.06	-1.88 (SCE)	
SBF [21]		Tris	380	-1.97 (SCE)	212
SBF [12]		Tris	31.6	-1.71 (Ag/AgCl)	1438
Hanks [22]		Tris & HCl	400	-1.85 (SCE)	180
SBF-1 [23]	air	Tris-HCl/HCO <sub>3</sub> <sup>-</sup>	300	-1.97 (SCE)	133
SBF-2 [23]	air	Tris-HCl/HCO <sub>3</sub> <sup>-</sup>	398	-1.96 (SCE)	464
SBF-3 [23]	air	Tris-HCl/HCO <sub>3</sub> <sup>-</sup>	28.8	-1.71 (SCE)	1801
Hanks [24]		Citric acid-Na <sub>2</sub> HPO <sub>4</sub>	250	-1.8(SCE)	30 (5 days) 2500 (30 days)

**Table 3.** Chemical composition of magnesium.

<b>Element</b>	<b>Zn</b>	<b>Ca</b>	<b>Fe</b>	<b>Cu</b>	<b>Al</b>	<b>Mn</b>	<b>Si</b>	<b>Mg</b>
<b>Weight %</b>	0.008	0.003	0.004	0.001	0.007	0.002	0.01	99.965

**Table 4.** EIS fitting results for pure magnesium samples in EBSS, EBSS+CO<sub>2</sub>, and EBSS with different concentrations of HEPES.

Elements	EBSS	EBSS+CO <sub>2</sub>	EBSS + HEPES 25 mM	EBSS + HEPES 50 mM	EBSS + HEPES 100 mM
<b>CPE<sub>1</sub></b> ( $\Omega^{-1} \cdot \text{cm}^{-2} \cdot \text{s}^{-n} \times 10^{-6}$ )	7 ± 2	23	68 ± 8	145 ± 86	235 ± 180
<b>n</b>	0.66	0.61	0.57	0.70	0.59
<b>R<sub>1</sub></b> ( $\Omega \text{ cm}^2$ )	962 ± 299	289	183 ± 69	136 ± 22	62 ± 12
<b>CPE<sub>2</sub></b> ( $\Omega^1 \cdot \text{cm}^2 \cdot \text{s}^{-n} \times 10^{-6}$ )	6 ± 0.8	12	18 ± 5	35935 ± 7237	8102 ± 11450
<b>n</b>	0.92	0.92	0.88	0.93	0.99
<b>R<sub>2</sub></b> ( $\Omega \text{ cm}^2$ )	45363 ± 6126	9573	870 ± 29	7 ± 4	28 ± 29

**Table 5.** Electrochemical data for pure magnesium in EBSS, EBSS+CO<sub>2</sub>, and EBSS with different concentrations of HEPES.

<b>Medium</b>	<b>E<sub>corr</sub></b> <b>(V<sub>(Ag/AgCl)</sub>)</b>	<b>i<sub>corr</sub></b> <b>(μA/cm<sup>2</sup>)</b>	<b>E<sub>bd</sub></b> <b>(V<sub>(Ag/AgCl)</sub>)</b>	<b>i<sub>(-1.45 V)</sub></b> <b>(μA/cm<sup>2</sup>)</b>
<b>EBSS</b>	-1.57 ± 0.01	1.03 ± 0.06	-1.4	5.36 ± 0.46
<b>EBSS + CO<sub>2</sub></b>	-1.55 ± 0.13	6.25 ± 2.5	-1.45	17.89 ± 18.18
<b>EBSS + HEPES 25mM</b>	-1.71 ± 0.17	28.5 ± 6.42	-1.4	315 ± 74.95
<b>EBSS + HEPES 50mM</b>	-1.77 ± 0.2	166 ± 8.18	-1.35	934
<b>EBSS+ HEPES 100mM</b>	-1.79 ± 0.22	243.67 ± 5.84	-	1263

**Table 6.** pH of the exposed medium before and after potentiodynamic polarisation (PP) experiments.

<b>solution</b>	<b>pH (before PP)</b>	<b>pH (after PP)</b>
<b>EBSS</b>	7.61±0	8.14±0.01
<b>EBSS+CO<sub>2</sub></b>	7.63±0.05	7.85±0.05
<b>EBSS+HEPES 25mM</b>	7.45±0.03	7.71±0.10
<b>EBSS+HEPES 50mM</b>	7.49±0.03	7.91±0.19
<b>EBSS+HEPES 100mM</b>	7.44±0.06	7.71±0.11